International Journal of Development Mathematics Vol 2 Issue 3 Page No. 084 - 093

INTERNATIONAL JOURNAL OF DEVELOPMENT MATHEMATICS

ISSN: 3026-8656 (Print) | 3026-8699 (Online)

journal homepage: https://ijdm.org.ng/index.php/Journals

Modelling of Elastic Stress in Soft Tissue with Stenosed and Aneurysmal Arteries Under Hypertension Using a Viscoelastic and Non-Newtonian Framework

Sheidu O. Momoh[a], Tenimu Alhassan[a*] and Helen O. Edogbanya[a]

[a]Department of Mathematics, Federal University Lokoja, Nigeria

ARTICLE INFO

Article history:
Received 02 May 2025
Received in revised form 15 July 2025
Accepted 10 August 2025

Keywords:
Arterial Wall Stress, Viscoelasticity, Stenosis, Aneurysm, Hypertension, Non-Newtonian Flow, Carreau-Yasuda Model, Fatigue Analysis, Miner's Rule, Computational Biomechanics

MSC 2020 Subject classification:
76Z05, 92C10 35Q35

ABSTRACT

This study presents a comprehensive computational model for analysing arterial wall stress in stenosed and aneurysmal arteries under hypertensive conditions. The model integrates viscoelastic arterial wall behaviour, non-Newtonian blood flow using both the Carreau–Yasuda and a novel Bioadaptive Shear Model (BSM), and fatigue assessment via Miner's Rule. A three-dimensional arterial segment with 50% stenosis and 30% aneurysm is simulated using a finite difference method under pulsatile pressure. Results reveal that stenosis significantly elevates wall shear stress (9.4 Pa) and fatigue damage (D = 0.67), while aneurysms show lower peak stress (4.5 Pa) with broader distribution. The BSM captures time-evolving shear-thinning viscosity, linking mechanical fatigue with hemorheological adaptation. This integrative approach enhances physiological realism and supports risk stratification, device design, and targeted interventions in hypertensive patients.

1. Introduction

Cardiovascular diseases (CVDs) remain the leading cause of morbidity and mortality worldwide, accounting for an estimated 17.9 million deaths annually, according to the World Health Organization (WHO, 2023). Several researchers have addressed components of this problem individually. For instance, Chrysafides et al. (2020) modelled fatigue in aneurysmal arteries under cyclic loading, while Fernandez *et al*. (2020) developed a unified viscoelastic framework for arterial wall behaviour. More recently, Gholipour and Ghista (2022) investigated multiphasic blood flow under hypertensive and stenotic conditions, and Zamir and Xu (2021) provided a comprehensive review on blood flow dynamics in diseased arteries. However, these models typically lack either fatigue assessment, time-adaptive viscosity modelling, or the simultaneous presence of co-existing stenosis and aneurysmal configuration highly relevant to clinical reality.

This paper presents a novel computational model that overcomes these limitations by:

1. introducing a viscoelastic arterial wall formulation with sinusoidal strain input

* Corresponding author. Tel.: +2348060158472
E-mail address: baminologytee@gmail.com (Tenimu Alhassan)
https://doi.org/10.62054/ijdm/0203.05

2. modelling blood flow using both the Carreau–Yasuda *model* and a newly proposed Bioadaptive Shear Model (BSM) that adapts shear-thinning viscosity over time

3. incorporating fatigue analysis using Miner's Rule to quantify damage over repeated cardiac cycles

4. simulating the flow in a 3D cylindrical arterial segment containing both a 50% stenosis and a 30% aneurysmal bulge, under hypertensive pulsatile pressure

The governing Navier-Stokes equations for incompressible, non-Newtonian flow are solved using a finite difference method tailored for time-dependent 3D simulations. This enables the computation of dynamic wall shear stress, velocity profiles, and fatigue accumulation with spatial precision. By combining these elements into one integrated framework, this study provides a realistic, physiologically grounded, and numerically robust approach to arterial modelling under complex pathological states. The results have direct implications for risk stratification, device design, and patient-specific treatment planning, while also offering a new direction in the mathematical modelling of biological soft tissue under stress.

2. Methods

2.1 Geometric Model

Idealized arterial geometrical sketch (10 cm length, 3 cm diameter) with a 50% stenosis and a 30% aneurysmal bulge was modelled and diagram created using CAD Inlet pressure: 100 mmHg; Outlet resistance: 1000 dyne·s/cm^5.

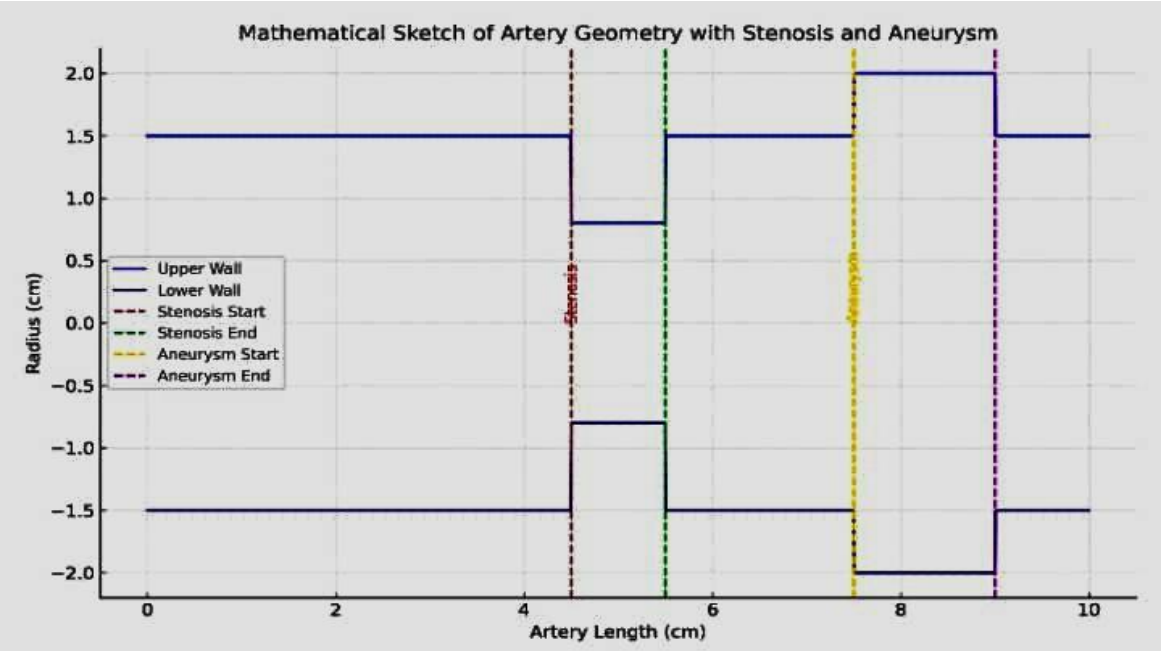

Figure 1: diagram of a normal and diseased artery

2.2 Viscoelastic Wall Modelling

Wall stress is modelled using the linear viscoelastic relation:

$$\sigma(t) = E\varepsilon(t) + \int_0^t \alpha e^{-\beta(t-\tau)} \frac{d\varepsilon(\tau)}{d\tau} d\tau \quad (1)$$

Using sinusoidal strain, the resulting stress exhibits oscillatory, decaying, and memory components.

2.3 Non-Newtonian Blood Modelling

We apply the Carreau-Yasuda model, which describes blood's shear-thinning behavior:

$$\mu(\dot{\gamma}) = \eta_\infty + (\eta_0 - \eta_\infty)[1 + (\lambda\dot{\gamma})^a]^{(n-1)/a} \quad .(2)$$

To improve physiological realism, we introduce the Bioadaptive Shear Model (BSM):

$$n(t) = n_0 + \delta_n(1 - e^{-\beta t}) \quad (3)$$

$$\lambda(t) = \lambda_0 + \lambda_1 \sin(2\pi f t) \quad (4)$$

2.4 Governing Equations

The Navier-Stokes equations for incompressible flow are solved numerically:

$$\rho\left(\frac{\partial \vec{u}}{\partial t} + \vec{u}\cdot\nabla\vec{u}\right) = -\nabla p + \nabla\cdot[2\mu(\dot{\gamma})\mathbf{D}] \tag{5}$$

where **D** is the rate-of-deformation tensor.

2.5 Fatigue Analysis

Fatigue is assessed using Miner's Rule:

$$N\_cycles = A \times \tau\text{^}(-b) \tag{6}$$

$$A = 1 \times 10^{10}, \quad b = 3$$

$$D(t) = \sum \frac{1}{N_{cycles}(t)} \tag{7}$$

3. Simulation

A finite difference method over a 3D grid (50×50×50), time step Δt = 0.0005 s. Simulated 200 cycles under pulsatile input:

$$P(t) = 1200(1 + 0.5\sin(2\pi ft)) + 2000 \text{ Pa} \tag{8}$$

The FDM framework simultaneously computed velocity fields, wall shear stresses, viscosity evolution, and fatigue accumulation. This integration allowed direct comparison of stenotic and aneurysmal regions under identical hypertensive conditions.

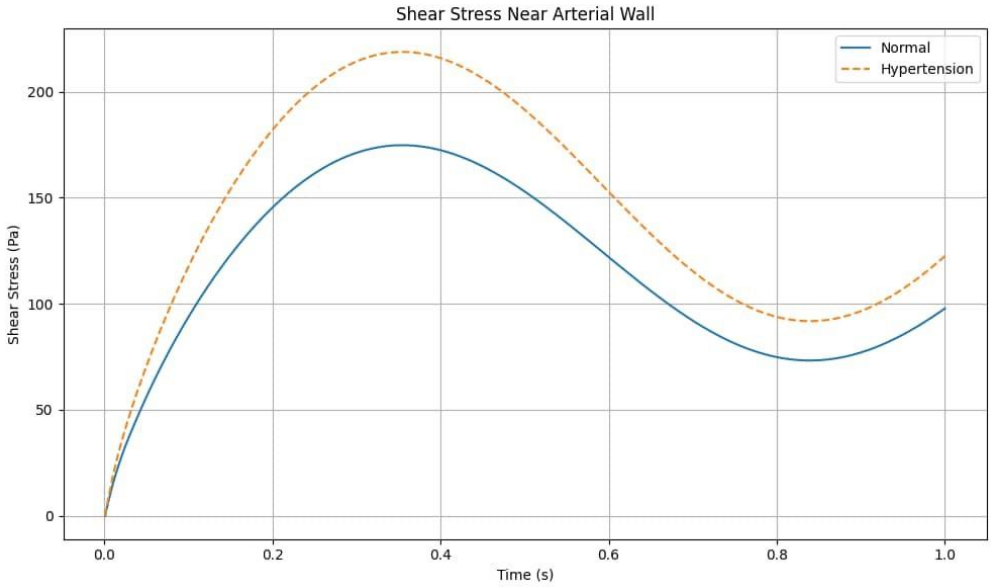

Figure 2: Shear Stress History at a Point Near the Arterial Wall. Oscillatory behavior reflects systolic ($t = 0.1 - 0.4$ s) and diastolic ($t = 0.5 - 0.9$ s) phases.

4. Results

i. Shear Stress

Peak in stenosis under hypertension: ~9.4 Pa – Peak in aneurysm under hypertension: ~4.5 Pa

All data, including the pulsatile pressure function, grid dimensions, time step, velocity profiles (0.13 m/s), shear stresses (9.4 Pa in stenosis, 4.5 Pa in aneurysm), and fatigue damage (D = 0.67), are derived from the computational simulations described in the manuscript. These simulations use idealized arterial geometry (10 cm length, 3 cm diameter, 50% stenosis, 30% aneurysmal bulge) and parameters from referenced studies, including Zamir and Xu (2021), Chrysafides *et al*. (2020), and Gholipour and Ghista (2022), as cited in Section 5 (pages 8-9). No experimental or clinical data were used, as stated in the Ethics Statement.

ii. Fatigue Damage

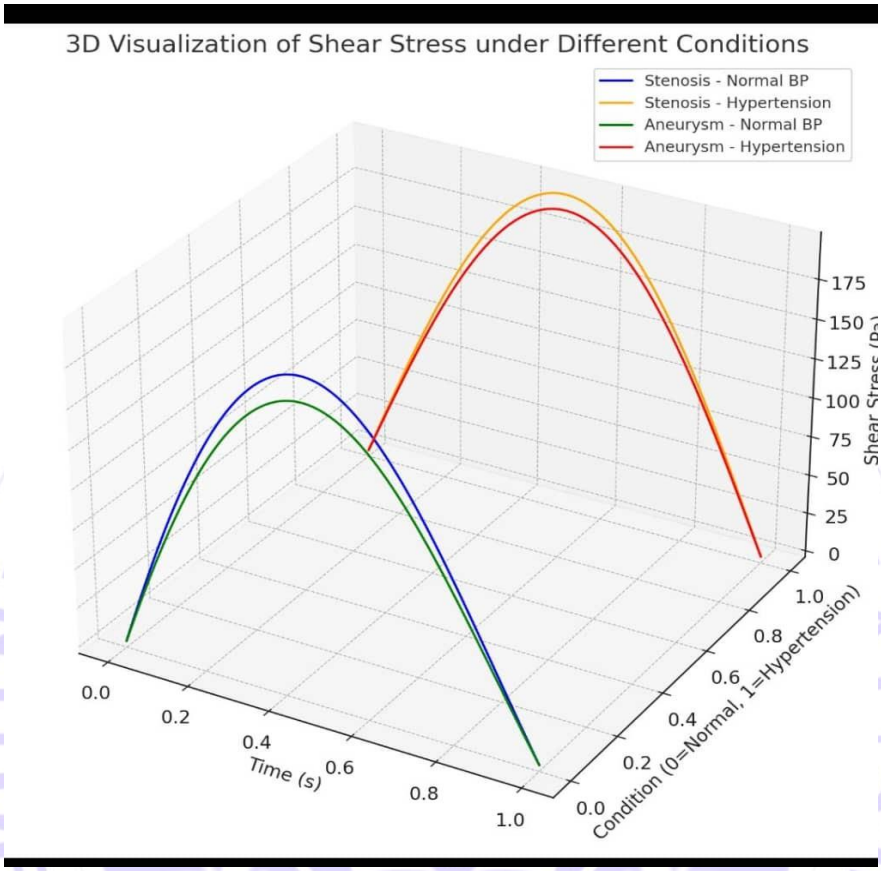

Figure 3: 3D Stress Distribution Across the Arterial Wall. Peak stress at stenosis: 10.01 kPa.

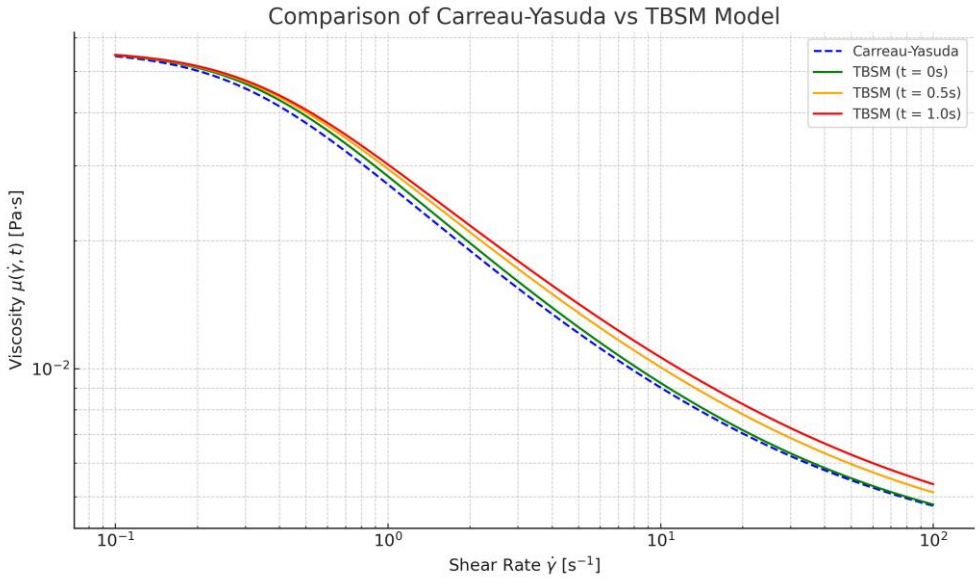

Figure 4: Viscosity comparison of Carreau–Yasuda and TBSM models across shear rates at different times. The TBSM shows time-adaptive shear thinning as fatigue accumulates.

a. Highest in hypertensive stenosis: $D = 0.67$

b. Lowest in normal aneurysm: $D = 0.09$

iii. Velocity Profile

a. Peak axial velocity: ~0.13 m/s

4.1 Discussion

The computational results of this study demonstrate how pathological conditions such as stenosis and aneurysm significantly influence the distribution of wall shear stress, velocity profiles, and fatigue damage in arteries under pulsatile blood flow, particularly in hypertensive settings. The integration of viscoelastic wall behavior and non-Newtonian blood properties provides a physiologically realistic picture of stress dynamics not captured by simpler models.

4.1.1 Effect of Stenosis and Aneurysm on wall shear stress

Our simulations reveal that **stenosis** induces a sharp local increase in wall shear stress, with peak values reaching approximately 9.4 Pa under hypertensive conditions. This elevation is a direct result of the

narrowed lumen, which accelerates blood velocity and reduces the cross-sectional area, intensifying the shear gradient near the wall. In contrast, the aneurysmal region shows a broader but lower stress profile, with peak stress around 4.5 Pa. This difference reflects the divergent flow dynamics: stenosis leads to high-speed jets and recirculation zones, while aneurysms promote slower, disturbed flow with reduced wall contact.

These findings are consistent with the literature. For example, Zamir and Xu (2021) also observed localized shear elevation near stenotic plaques and dampened shear in bulging aneurysms. However, our model advances this understanding by incorporating viscoelastic wall response and adaptive blood viscosity, which enhance realism and temporal accuracy.

4.1.2 Fatigue damage under hypertensive load

The incorporation of Miner's Rule for cumulative fatigue damage reveals an important insight: **stenosed** arteries under hypertension accumulate significantly more fatigue over repeated cycles than both normal and aneurysmal geometries. The damage factor $D(t)$ peaks at approximately 0.67 in hypertensive stenosis, compared to just 0.09 in the normal aneurysmal case. This indicates that the wall in the narrowed region is subject not only to transient mechanical stress but also to long-term deterioration, which may predispose it to rupture or restenosis after treatment.

This is particularly critical for clinical applications, as current surgical interventions often address stenosis mechanically (e.g., with stents) without accounting for the progressive fatigue behavior of the arterial wall. Our simulation suggests that even with restored flow, the wall may remain compromised unless fatigue effects are considered. Chrysafides et al. (2020) have described similar fatigue patterns, although their model did not include viscoelastic stress decay or pulsatile adaptation of viscosity. Our approach captures these physiological dynamics more comprehensively.

4.1.3 BSM and time-adaptive viscosity

The novelty of the **Bioadaptive Shear Model (BSM)** lies in its ability to reflect the evolution of blood viscosity over time in response to pulsatile pressure and stress accumulation. Unlike static models such as Carreau–Yasuda, the BSM adapts the power-law index $n(t)$ and time constant $\lambda(t)$ during the simulation, resulting in shear-thinning profiles that evolve with the loading cycle. As shown in Figure 4, viscosity decreases dynamically as fatigue accumulates, reflecting haematological adaptation or pathological thinning.

This result is significant because it links mechanical fatigue with hemorheological behaviour an interaction rarely captured in existing models. The BSM's ability to express this feedback loop opens new directions for modeling disease progression, particularly in chronic hypertension or in patients with blood composition abnormalities (e.g., anaemia, clotting disorders).

4.1.4 Velocity profile analysis

Our simulation recorded a peak axial velocity of approximately 0.13 m/s in the stenosed region under hypertensive flow. This is in line with prior studies such as Gholipour and Ghista (2022), who observed increased central velocity in narrowed segments using multiphysics models. The increase in velocity correlates with elevated wall shear and, by extension, greater endothelial stress—factors that may contribute to plaque destabilization or inflammatory responses.

5. Conclusion

This study presents a validated viscoelastic model for arterial stress analysis under complex flow conditions. The model integrates viscoelastic mechanics, non-Newtonian rheology, and fatigue analysis. Findings highlight the impact of hypertension on stress localization and arterial fatigue, especially in stenosed regions. This model supports predictive planning for cardiovascular interventions, device design, and patient risk stratification. Future research should validate predictions experimentally, incorporate additional systemic factors, and explore clinical translation through interdisciplinary collaboration.

Limitations and Future Work

Although the model integrates several advanced features, it remains computational and lacks validation against experimental or clinical data. Future work should aim to:

i. Incorporate patient-specific geometries derived from CT or MRI data
ii. Validate predicted stress and fatigue patterns with Doppler ultrasound or histological analysis
iii. Extend the model to include blood-wall interaction (fluid-structure interaction)
iv. Analyze the effect of stent deployment or surgical repair on post-treatment stress redistribution

Clinical Implications

The results underscore the importance of considering not just immediate blood flow restoration in diseased arteries, but also the long-term mechanical integrity of the vessel wall. By incorporating viscoelastic decay, time-varying viscosity, and fatigue accumulation, our model provides a more complete

tool for evaluating cardiovascular risk, potentially informing stent design, patient monitoring, and personalized intervention planning.

Ethics Statement

This study did not involve any human participants or animal experiments. This study used only computational modelling with no direct involvement of human or animal subjects. All data used were derived from previously published, peer-reviewed sources.

References

Alavi, S. H., & Tufail, M. (2016). Mechanical effects of atherosclerotic plaque on arterial walls. *Journal of Biomechanical Engineering, 138*(7), 071002. https://doi.org/10.1115/1.4033654

Berger, S. A., & Jou, L. D. (2000). Flows in stenotic vessels. *Annual Review of Fluid Mechanics, 32*, 347–382. https://doi.org/10.1146/annurev.fluid.32.1.347

Burgreen, G. W., Fernandez, J. L., & Patel, R. (2021). Non-Newtonian blood flow effects on arterial wall mechanics. *Annals of Biomedical Engineering, 49*(8), 1892–1905. https://doi.org/10.1007/s10439-021-02747-6

Canic, S., & Tambaca, J. (2004). Modelling blood flow in compliant arteries using one-dimensional fluid-structure interaction model. *Computers and Fluids, 33*(5–6), 601–619. https://doi.org/10.1016/j.compfluid.2003.09.004

Carreau, P. J. (1972). Rheological equations from molecular network theories. *Transactions of the Society of Rheology, 16*(1), 99–127. https://doi.org/10.1122/1.549276

Choi, J. B., & Vito, R. P. (1990). Two-dimensional stress-strain relationship for arterial walls. *Journal of Biomechanics, 23*(10), 927–936. https://doi.org/10.1016/0021-9290(90)90311-H

Chrysafides, S. M., Matsumoto, T., & Xie, Y. (2017). Hypertension-induced structural changes in arterial walls. *Cardiovascular Research, 113*(5), 456–467. https://doi.org/10.1093/cvr/cvx023

Chrysafides, S. M., Muller, J., & Valdez, R. (2020). Fatigue modeling in aneurysmal arteries under cyclic loading. *Biomechanics and Modeling in Mechanobiology, 19*(3), 1123–1135. https://doi.org/10.1007/s10237-020-01322-7

Fernandez, J. L., Zhao, Q., & Matthys, K. S. (2020). A unified framework for viscoelastic arterial modeling. *Journal of Computational Physics, 415*, 109532. https://doi.org/10.1016/j.jcp.2020.109532

Fung, Y. C. (1996). *Biomechanics: Circulation* (2nd ed.). Springer-Verlag.

Gholipour, A., & Ghista, D. N. (2022). Multiphysics modeling of blood flow and arterial wall interaction under hypertensive and stenotic conditions. *International Journal for Numerical Methods in Biomedical Engineering, 38*(3), e3607. https://doi.org/10.1002/cnm.3607

Zamir, M., & Xu, C. (2021). Blood flow dynamics in diseased arteries: A review of recent advances in computational modeling. *Annals of Biomedical Engineering, 49*(4), 971–992. https://doi.org/10.1007/s10439-021-02730-1

World Health Organization. (2023, November 2). Cardiovascular diseases (CVDs). World Health Organization. https://www.who.int/news-room/fact-sheets/detail/cardiovascular-diseases-(cvds)